DOI: 10.1002/cphc.200900345

Optical and Magnetic Properties of Conjugate Structures of PbSe Quantum Dots and γ-Fe_2O_3 Nanoparticles

Lioz Etgar,[d] Gregory Leitus,[e] Leonid Fradkin,[b, f] Yehuda G. Assaraf,[g] Rina Tannenbaum,*[a, c] and Efrat Lifshitz*[b]

An investigation of the optical and magnetic properties of a unique hydrogen-linked conjugate nanostructure, comprised of superparamagnetic γ-Fe_2O_3 nanoparticles (NPs) and near-infrared PbSe nanocrystal quantum dot (NQD) chromophores, is reported. The results show retention of the NQDs' emission quantum efficiency and radiative lifetime, and only a small red shift of its band energy, upon conjugation to the dielectric surroundings of γ-Fe_2O_3 NPs. The study also shows the sustainability of the superparamagnetism of the NPs after conjugation, with only a slight decrease of the ferromagnetic–superparamagnetic transition temperature with respect to that of the individual NPs. Thus, the conjugate nanostructure can be considered as a useful medical platform when PbSe NQDs act as fluorescent tags, while the γ-Fe_2O_3 NPs are used as a vehicle driven by an external magnetic field for targeted delivery of tags or drugs.

1. Introduction

An important research area in the field of nanomaterials is the expansion from a single material into conjugate nanoscale or mesoscale structures with discrete domains of different materials.[1–3] These conjugate structures are expected to exhibit unique properties due to the integration of different functionalities, by retaining the capabilities of the individual components and optimization of the conjugate's physical parameters.

This study concentrates on the investigation of the distinctive optical and magnetic properties of conjugate nanostructures consisting of superparamagnetic γ-Fe_2O_3 nanoparticles (NPs) and near-infrared PbSe nanocrystal quantum dot (NQD) chromophores (referred to as NQD–NP conjugates). The components were capped with selective surfactants, chosen to permit hydrogen linking and promote solubility in aqueous solutions, which were compatible with the biological environment. The properties of these conjugate structures give them considerable importance as a new class of multifunctional nanoscale structures,[4] particularly in their adaptability for biolabeling/imaging and cell sorting/separation.[5] In these conjugate nanostructures, the magnetic NPs may serve as transport vehicles (nanoplatforms) that could be manipulated by an external magnetic field gradient, and the NQDs may act as fluorescent tags in the near-infrared regime, thereby allowing an optical window for in vivo cancer-cell detection. Furthermore, the conjugate structures could be functionalized with biorecognition molecules that would be selectively targeted to a biological target, and hence would be compatible with personal medical applications. The magnetic-semiconductor conjugate can also be equipped with drug molecules to be released at the specific site of the cancer cells, for the simultaneous targeted therapy of the labeled target.

The NQDs exhibit characteristic electronic and optical tunability that varies according to their size. Currently, PbSe NQDs are the focus of extensive attention due to their distinctive intrinsic properties,[6–8] and show well-defined band-edge excitonic transitions tuned between 1 and 3.5 μm emission with an optical penetration depth in living tissue of 5–10 cm,[9] a relatively large ground-state cross section of absorption (~10^{-15} cm^{-2}), long excitonic lifetime at room temperature (400–500 ns), and exceptionally high room-temperature luminescence quantum efficiency (~80%),[10–12] altogether making them suitable as fluorescing tags in biological applications.[13–15]

The γ-Fe_2O_3 NPs have physical and chemical properties that are not characteristic of either their discrete (atomic) or their

---

[a] Prof. R. Tannenbaum
Department of Chemical Engineering
Technion, Haifa 32000 (Israel)
Fax: (+972) 48292850
E-mail: rinatan@technion.ac.il

[b] Dr. L. Fradkin, Prof. E. Lifshitz
Schulich Faculty of Chemistry
Solid State Institute, Russell Berrie Nanotechnology Institute
Technion, Haifa 32000 (Israel)
Fax: (+972) 48235107
E-mail: ssefrat@technion.ac.il

[c] Prof. R. Tannenbaum
School of Materials Science and Engineering
Georgia Institute of Technology, Atlanta, GA 30332(USA)

[d] L. Etgar
Nanoscience and Nanotechnology Program
Technion, Haifa 32000 (Israel)

[e] Dr. G. Leitus
Chemical Research Support Department
Weizmann Institute of Science, Rehovot 76100 (Israel)

[f] Dr. L. Fradkin
Center for Nano- and Molecular Science and Technology
The University of Texas at Austin (USA)

[g] Prof. Y. G. Assaraf
The Fred Wyszkowski Cancer Research Laboratory
Department of Biology, Technion, Haifa 32000 (Israel)

© 2009 Wiley-VCH Verlag GmbH & Co. KGaA, Weinheim

bulk counterparts.[16,17] Quantum size effects and the large surface area of these magnetic NPs dramatically change some of their magnetic properties, such as the exhibition of both superparamagnetic properties and quantum tunneling of magnetization. Based on their unique mesoscopic physical, tribological, thermal, and mechanical properties, these superparamagnetic NPs offer great potential in several applications including ferro fluids, color imaging, magnetic refrigeration, detoxification of biological fluids, magnetically controlled transport of anticancer drugs, magnetic resonance imaging, contrast enhancement, and magnetic cell separation.[18–21]

The optical properties of the NQD–NP conjugates were measured by monitoring their continuous-wave photoluminescence (cw-PL) spectra with/without the influence of an external magnetic field and their PL decay curves, in comparison with processes occurring in the free NQDs under the same conditions. The magnetization of the NQD–NP conjugate was examined by a superconducting quantum interference device (SQUID), and evaluated with respect to the magnetization of the free NPs. As discussed below, the presence of adjacently coupled species induced only a fine-tuning of the optical and magnetic properties of the individual components, which suggests retention of the integrated functionalities within the conjugate structure.

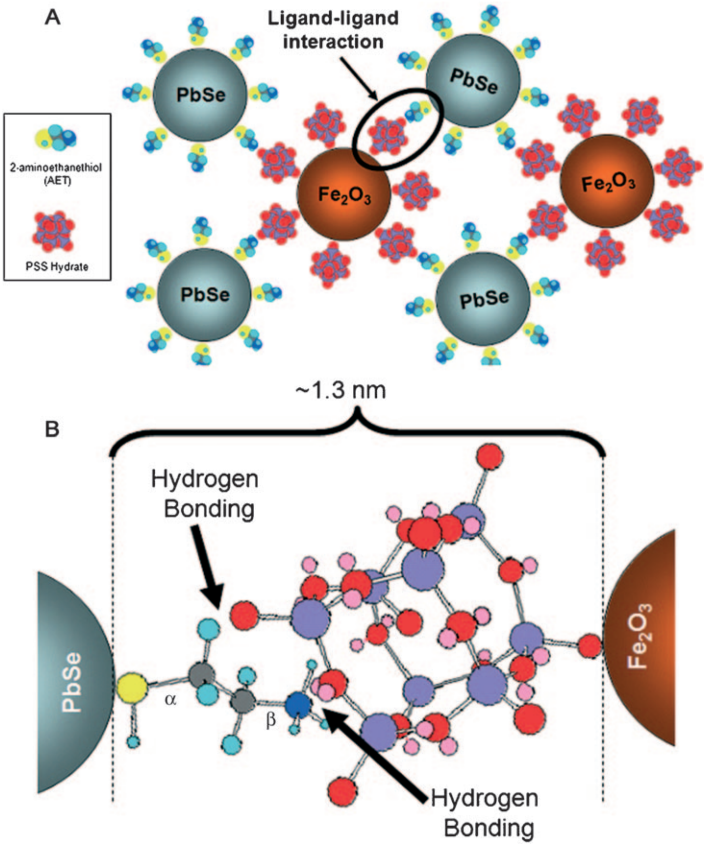

Figure 1. A) γ-Fe_2O_3 NPs functionalized by hydrophilic PSS ligands containing eight SiO^- functional groups. B) Equivalent amounts of NQDs and NPs in acidic solution permit ligand–ligand interaction via a hydrogen bond between the NH_3^+ and SiO^- functional groups. (● thiol, ● oxygen, ● hydrogen, ● silicon, ● nitrogen, ● carbon, ● nonbonding electrons.)

2. Results and Discussion

The free PbSe NQDs and the γ-Fe_2O_3 NPs, with a typical diameter of ~5 nm, were synthesized by colloidal procedures (see Experimental Section). The PbSe NQDs were functionalized by 2-aminoethanethiol (AET) surfactant, with the amino groups facing the exterior periphery. The γ-Fe_2O_3 NPs were functionalized by hydrophilic polyhedral silsesquioxane (PSS) ligands containing eight SiO^- functional groups (see Figure 1 A). A mixture of equivalent amounts of NQD and NP constituents in acidic solution (pH~5) permits ligand–ligand interaction via hydrogen bonds between the NH_3^+ and SiO^- functional groups, as shown in Figure 1 B. Previous energy minimization calculations (using Gaussian 98 commercial-software)[22] revealed the occurrence of an additional hydrogen bridge between an adjacent SiO^- group and a $-CH_2-$ fragment in the AET (Figure 1 B). These double hydrogen bridges reduced the enthalpy of the system from 1077 to 699 kcal mol^{-1} e.[22]

Figure 2 A presents a transmission electron microscopy (TEM) image of PbSe NQD–γ-Fe_2O_3 NP conjugates deposited onto a TEM grid from an acidic solution at pH ~ 5, which shows clustering of particles. The corresponding electron diffraction pattern (Figure 2 A, inset) reveals the existence of PbSe (space group $Fm\bar{3}m$) and γ-Fe_2O_3 (space group $P4_132$) particles within a cluster. Furthermore, a zoom view over a single cluster (Figure 2 B) reveals distinctive lattice fringes of the individual NQDs and NPs, with a surface-to-surface distance of 1.3 nm between adjacent particles, in good agreement with the combined AET–PSS molecular length, thus supporting the formation of a hydrogen bond (Figure 1 B).

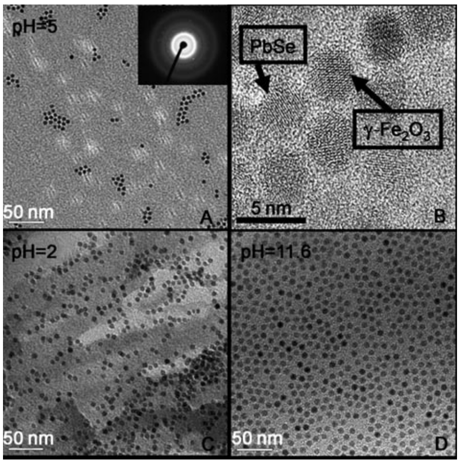

Figure 2. A) TEM image of PbSe NQD–γ-Fe_2O_3 NP conjugates, deposited from a solution of pH ~ 5, and the corresponding electron diffraction pattern (inset). B) Zoom view over a single cluster, with arrows indicating individual NQD and NP particles, at a mutual surface-to-surface distance of 1.3 nm. C, D) TEM images of NQD/NP mixtures, deposited from a water solution of pH 2 (C) and pH 11.6 (D), which show dispersion of the particles.

© 2009 Wiley-VCH Verlag GmbH & Co. KGaA, Weinheim

Figures 2 C and D show TEM images of NQD/NP mixtures deposited onto a TEM grid from a water solution of pH 2 and 11.5, respectively. These images reveal a random dispersion of the individual particles, which avoids conjugation of the particles, under extreme acidic/basic conditions. More likely, a strongly acidic solution protonizes the SiO^- groups whereas a strongly basic solution deproponizes the NH_3^+ group, both blocking the ligand–ligand interactions. It appears, therefore, that the extent of conjugation between the PbSe NQDs and the γ-Fe_2O_3 NPs can be controlled by the pH of the suspension in which this process takes place, thus supplying further evidence for hydrogen bonding between the NQD and NP components. It is noted that the pH stability of the conjugates would have to be controlled when used as a medical platform.

Figure 3 shows the ^1H NMR spectra of AET-capped PbSe NQDs (blue curve) and their mixture with PSS molecules (red curve), both recorded in D_2O solution. The spectrum of the AET-capped NQDs is dominated by two triplet resonances, centered at 2.77 and 2.43 ppm, related to the $-CH_2-$ bonds labeled in Figure 1 B as α and β, respectively. The labile protons on the NH_3^+ unit are more likely exchanged by the surrounding deuterium atoms, thus making them invisible in the ^1H NMR spectrum. Furthermore, the discussed triplet resonances appear at lower chemical shifts, α at 2.38 ppm and β at 2.18 ppm, upon mixing with the PSS molecules. This change is related to electron screening induced by a SiO^- unit of the PSS moieties in the vicinity of both the α and β protons (when the influence on the β proton may be bridged via the amine group). Thus, the ^1H NMR spectra further support the occurrence of two hydrogen links between the AET and PSS functional molecules (Figure 1 B). Note that examination of the ^1H NMR spectrum in the presence of γ-Fe_2O_3 NPs showed a substantial broadening of the resonance bands (not shown), due a magnetic screening induced by the magnetic/metallic NPs, which avoided resolution of delicate changes in the chemical shifts.

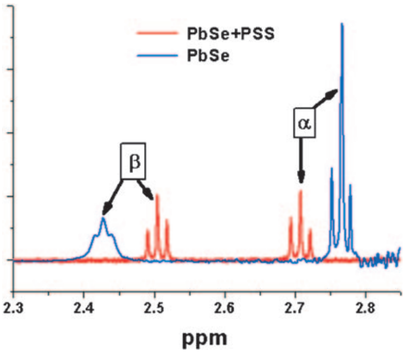

Figure 3. ^1H NMR spectra of AET-capped PbSe NQDs (blue curve) and their mixture with PSS molecules (red curve), both recorded in D_2O solution.

Figure 4 shows the cw-PL spectra of PbSe NQD–γ-Fe_2O_3 NP conjugates (red curves) and of free PbSe NQDs (blue curves), recorded at room temperature (bottom), at 1.4 K (middle), and at 1.4 K with the additional influence of an external magnetic field of 3×10^4 Oe (top). The spectra are composed of a single band, associated with the ground-state exciton emission with a quantum efficiency of 27 % (at room temperature). The exciton band of PbSe NQDs, either as free particles or within the conjugate nanostructure, is red-shifted upon cooling from room temperature to 1.4 K, a known effect in a bulk narrow-band semiconductor[23] and in colloidal PbSe NQDs.[24] The temperature shift is related to lattice dilatation, phonon coupling, and the dominancy of dark exciton emission in NQDs (at 1.4 K).

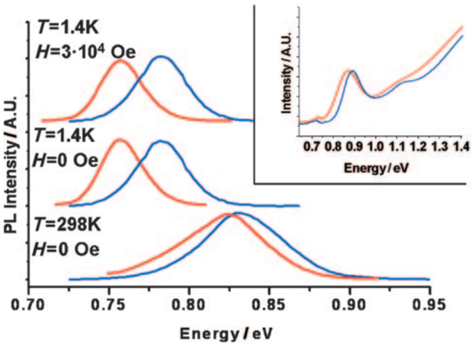

Figure 4. Representative PL spectra of individual PbSe NQDs (blue curves) and of the NQD–NP conjugates (red curves). The spectra were recorded at room temperature (bottom), at 1.4 K (middle), and at 1.4 K in the presence of an external magnetic field of 3×10^4 Oe (top). Inset: the corresponding absorption spectra of individual PbSe NQDs (blue curve) and NQD–NP conjugates (red curve). The average diameters of the NQDs and NPs were 5 nm.

Representative absorption spectra of the free 5 nm PbSe NQDs and the corresponding NQD–NP conjugate are shown in the inset of Figure 4, which exhibits nearly identical curves but with a red shift of the conjugate's spectrum by 12 meV with respect to that of the individual NQDs. This result is in comparison with a red shift of 14 meV between the room-temperature emission bands, presented as the bottom curves in Figure 4. The discussed energy difference increases with a decrease of the NQD radius (between 5 and 50 meV), and is correlated with the influence of the dielectric environment on the optical band gap. The dielectric environment is a function of the relative volume fraction of the γ-Fe_2O_3 NPs and water molecules in the immediate vicinity of the NQDs. Thus, the exciton red shift induced by the conjugation can be described by Equation (1):[25]

$$E_{\mathrm{gap}}^{\mathrm{opt}} = E_{\mathrm{gap}}^{\mathrm{qp}} - J_{\mathrm{e-h}} \tag{1}$$

The quasiparticle gap, $E_{\mathrm{gap}}^{\mathrm{qp}}$, is correlated with the energy difference between the lowest-energy kinetically confined electron and hole states, while $J_{\mathrm{e-h}}$ is related to the electron–hole Coulomb attraction energy and is given by Equation (2):[26]

$$J_{\mathrm{e-h}}(R) = \left(\frac{1}{\varepsilon_{\mathrm{out}}} + \frac{0.79}{\varepsilon_{\mathrm{in}}}\right)\frac{e^2}{4\pi\varepsilon_0 R} \tag{2}$$

where $\varepsilon_{\mathrm{in}}$ is the dielectric constant of the PbSe NQDs, R is the NQD radius, and $\varepsilon_{\mathrm{out}}$ is the weighted dielectric constant of the environment. Defining $J_{\mathrm{e-h}}^{\mathrm{water}}$ and $J_{\mathrm{e-h}}^{\mathrm{water+\gamma-Fe_2O_3}}$ as the Coulomb coupling energy in water and in water + γ-Fe_2O_3 environments, respectively, and considering the values $\varepsilon_{\gamma-Fe_2O_3} = 9.4$, $\varepsilon_{water} = 5.5$,[27] and $\varepsilon_{out} = \frac{(V_{\gamma-Fe_2O_3} \times \varepsilon_{\gamma-Fe_2O_3}) + (V_{water} \times \varepsilon_{water})}{V_{total}} = 6.67$ (V designates the corresponding volumes), the dielectric environment of the water-soluble PbSe NQDs alters upon conjugation with the metallic NPs, by the amount given in Equation (3):

$$\Delta J = J_{e-h}^{water} - J_{e-h}^{water+\gamma-Fe_2O_3} \tag{3}$$

The corresponding optical gap varies by the expression given in Equation (4):

$$\Delta E_{gap}^{opt} = E_{gap}^{opt,water} - E_{gap}^{opt,water+\gamma-Fe_2O_3} \tag{4}$$

The optical gaps (which nearly equate with the exciton emission energy) of free NQDs and their corresponding conjugates were measured for a set of samples with various NQD radii, while maintaining a constant ratio between the number of NQDs and NPs within a conjugate solution. The experimental ΔE_{gap}^{opt} versus the radius of the NQDs is plotted in Figure 5; the theoretical plot of ΔJ versus the diameter is given by the solid line. Although there is some deviation between the experimental and theoretical curves, the similar trend suggests that the dielectric surroundings induced by γ-Fe_2O_3 NPs have a major contribution to the red shift of the NQDs' exciton energy, without affecting the emission quantum efficiency. Also, the spectra recorded under the influence of an external magnetic field (top curves in Figure 4) did not show an obvious change with respect to its absence (middle curves). This point is important for future use in transferring the conjugates by a magnetic-field-driven process along a human vein (to be discussed elsewhere).

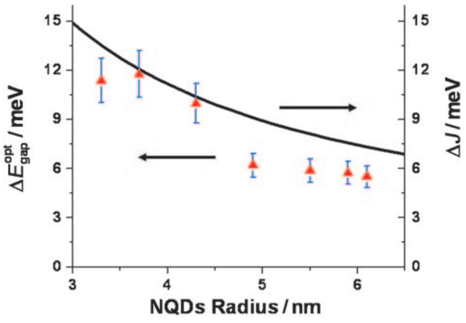

Figure 5. Observed shift ΔE_{gap} (triangles) and theoretical deviation ΔJ (solid line) of the emission band energy of PbSe NQDs upon their conjugation to γ-Fe_2O_3 NPs, plotted versus the NQD radius.

The PL decay curves of the free PbSe NQDs and the corresponding NQD–NP conjugate, recorded at room temperature, are illustrated in Figure 6. These decay curves were best fitted to a single exponential function, $I_{PL}(t) = A_1 \exp(-t/\tau_1)$, with a lifetime of 1056 and 905 ns for the free and conjugated NQDs, respectively. This small difference suggests a relatively weak electronic interaction between adjacent NQDs and metallic NPs. It is further supported by electron energy loss spectroscopy (EELS) measurements, which show a surface plasmon band of γ-Fe_2O_3 at ~24 eV (see Figure 7) in the free NPs and their conjugates. The plasmon energy is far from the band-edge electronic energy of the PbSe NQDs (located 4–5 eV below the vacuum level).[28,29] Thus, exciton–plasmon interactions that could lead to an electronic hybrid mixing or a Förster energy-transfer process[30] are completely eliminated in our case, thus avoiding the quenching of the luminescence process. Note that a lifetime of about a microsecond and resistance to quenchers permits comfortable biological detection, with the possibility to eliminate the autofluorescence background at this time range, and thus further supports the potential application of the NQD–NP conjugates in medical diagnostics.

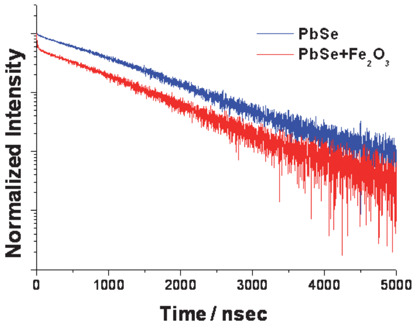

Figure 6. Normalized PL decay curves of the individual PbSe NQDs (blue) and the corresponding NQD–NP conjugates (red).

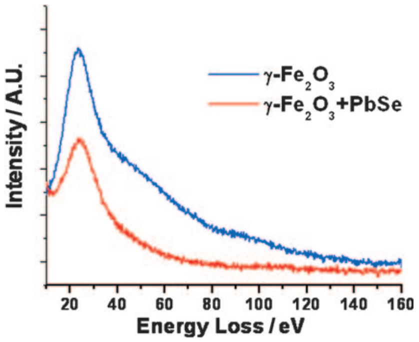

Figure 7. EELS spectra of a metallic plasmon of individual γ-Fe_2O_3 NPs (red curve) and NQD–NP conjugates (blue curve).

The magnetic properties of the NQD–NP conjugates were explored by following the change in the dc mass magnetic susceptibility of the conjugate structures as a function of temperature in comparison with that of free NPs. The susceptibility was measured from lower to higher temperatures after the sample was cooled in the presence/absence of an applied magnetic field of 500 Oe (field-cooled (FC)/zero-field-cooled (ZFC) magnetization). Representative susceptibility curves, recorded under FC and ZFC conditions, are shown in Figure 8. The intercept of the FC and ZFC curves corresponds to the blocking temperature T_b, a point at which the material under-

© 2009 Wiley-VCH Verlag GmbH & Co. KGaA, Weinheim

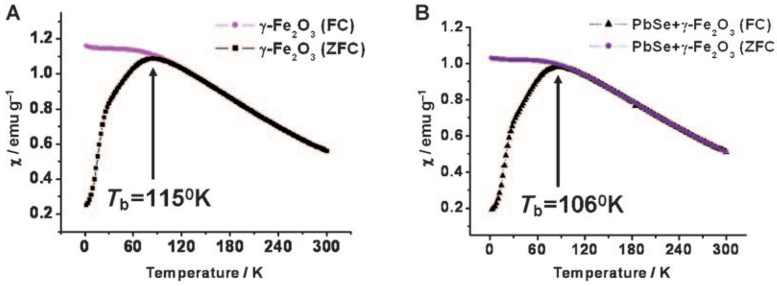

Figure 8. Plots of ZFC and FC magnetic susceptibility (χ) values, measured at $H = 500$ Oe, versus the temperature of the individual γ-Fe$_2$O$_3$ NPs (A) and of the PbSe NQD–γ-Fe$_2$O$_3$ NP conjugates (B), which show blocking temperatures (T_b) of 115 and 106 °K, respectively.

goes a magnetic phase transition from a ferromagnetic to a superparamagnetic material. Superparamagnetism depends on the critical size of a single domain structure, known to be about 15 nm in Fe crystals.[31] The present study focuses on γ-Fe$_2$O$_3$ NPs with an average diameter of 5 nm, which is close to the size of a single domain. The free γ-Fe$_2$O$_3$ NPs displayed a blocking temperature of 115 K (Figure 8 A), while the NQD–NP conjugates displayed a blocking temperature of 106 K (Figure 8 B). The reduction of T_b is associated with the mutual coupling between the conjugate constituents. The definition of T_b is expressed by Equation (5):[32,33]

$$T_b = (E_a + E_{int})/k_b \ln(tf_0) \tag{5}$$

where E_a is the anisotropy barrier, determined by $E_a = KV$ (K is the anisotropic energy density constant and V is the NP volume), f_0 is a frequency factor on the order of 10^9 s^{-1},[34] t is the experimental measuring time, and E_{int} is associated with the NP–NP interaction. Obviously, the change in the interaction of the NPs due to the integration of NQDs in their midst alters the interaction energy and T_b accordingly. A theoretical model considering the NP interactions as magnetic dipole–dipole coupling interactions has been presented by Dormann et al.[31,32], according to Equation (6):[31,35,36]

$$E_{int} \propto \frac{M^2}{r^3}(3\cos\psi_1 \cos\psi_2 - \cos\alpha) \tag{6}$$

where M is the magnetic moment of a NP, r is the distance between the NPs, ψ_1 and ψ_2 are the angles between r and the two moments, respectively, and α is the angle between the two moments. Thus, a reduction of the inter-NP distance increases the value of E_{int}. The interaction energy of the free γ-Fe$_2$O$_3$ NPs was calculated to be $E_{int} = 1.56 \times 10^{13}$ erg, and that of the NQD–NP conjugates was calculated as $E_{int} = 1.25 \times 10^{13}$ erg. This numerical evaluation reveals a reduction of the interaction energy among the magnetic NPs in the conjugated structures.

The magnetic susceptibility (χ) dependence on the strength of the external magnetic field (H) was determined at two different temperatures (20 and 300 K). Representative plots of this dependence of the free γ-Fe$_2$O$_3$ NPs and of the NQD–NP conjugates are shown in Figure 9 A and B, respectively. The $\chi(H)$ dependence measured at 20 K (below T_b) in both cases exhibits hysteretic behavior with pronounced coercivity, indicative of ferromagnetism at this temperature, whereas the $\chi(H)$ dependence measured at 300 K (above T_b) lacks the hysteretic behavior, and further supports the emergence of superparamagnetism and the retention of this property in the NQD–NP conjugates.

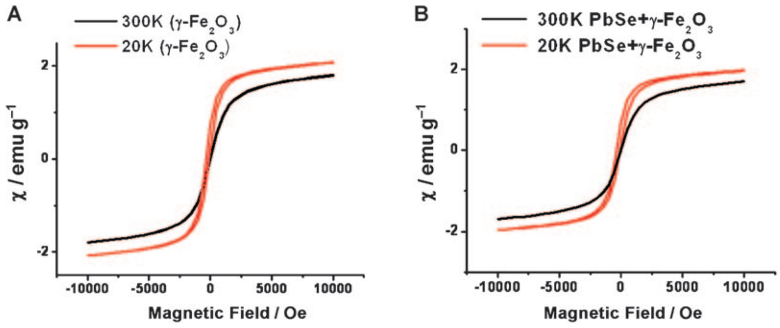

Figure 9. Plots of the magnetic susceptibility (χ) versus strength of an external magnetic field of the individual γ-Fe$_2$O$_3$ NPs (A) and of the PbSe NQD–γ-Fe$_2$O$_3$ NP conjugates (B). The plots were recorded at 20 and 300 K as indicated.

3. Conclusions

The properties of water-soluble conjugate structures consisting of magnetic NPs (γ-Fe$_2$O$_3$) attached to semiconductor NQDs (PbSe) were investigated and compared to those of the non-conjugated, individual components. The positively charged ligand-capped NQDs were bound to the negatively charged functional groups on the magnetic NPs by hydrogen bonds. The PL spectra of the conjugate structures showed a red shift of the exciton band compared to that of the free PbSe NQDs. This shift is associated with the dielectric screening induced by the metallic NPs. Despite this small red shift, the exciton energy of the conjugates does not change upon application of an external magnetic field; furthermore, the lifetime of the conjugates is nearly conserved with respect to that of the free NQDs. Magnetic measurements of the free NPs as well as the relevant conjugate structures showed a superparamagnetism behavior with a shift of the blocking temperature upon conjugation, due an increase of NP–NP distance with the inclusion of intermediate NQDs. Our results clearly indicated that the changes in the PL and magnetic properties were due to the

© 2009 Wiley-VCH Verlag GmbH & Co. KGaA, Weinheim

proximity of the NQDs and NPs achieved by their conjugation, and were not due to a random mixture of these NPs. This certitude arises from the fact that under the very specific mixing conditions of the components employed in our synthesis, shown to be dominated by the pH of the suspensions, the particles that are obtained are exclusively the NQD–NP conjugated nanostructures. Overall, the NQD–NP conjugates generally retained the physical properties and functionality of the constituents, essential information for their future use in several applications such as biosensing, detection of cancer cells, drug delivery, and spintronics.

Experimental Section

Synthesis of the Materials: The synthesis of individual PbSe NQDs, stabilized by organic surfactants [oleic acid (OA) and trioctylphosphine (TOP)], was reported in earlier studies.[37,38] This procedure produced nearly monodisperse NQDs with $<5\%$ size distribution and average sizes ranging between 3 and 9 nm, controlled by the reaction temperature and duration. The surfactant-stabilized PbSe NQDs were transferred into the water environment by exchanging the OA ligands with positively charged molecules of AET, by using a previously reported exchange procedure.[22]

The synthesis of individual γ-Fe$_2$O$_3$ NPs stabilized by organic surfactants (OA and TOP) was performed by a similar procedure to that described by Held et al.[39] The γ-Fe$_2$O$_3$ NPs were transferred into aqueous solution by replacing the organic ligands (OA) with negatively charged hydrated octakis(tetramethylammonium) ($C_{32}H_{96}N_8O_{20}Si_8{\cdot}x\,H_2O$)] molecules, known as hydrophilic PSS, through an exchange procedure similar to that given by Frankamp et al.[40]

The preparation of the NQD–NP conjugates involved the simple mixing of equal volumes of a water-based solution of the AET-capped PbSe NQDs with a water-based solution of the PSS-capped γ-Fe$_2$O$_3$ NPs in an acidic environment (pH ~ 5), as shown in Figure 1 A. Further details are discussed in a previous publication.[22]

Structural, Optical, and Magnetic Characterization: The chemical conjugation between the PbSe NQDs and the γ-Fe$_2$O$_3$ NPs was characterized by the use of pulsed NMR spectroscopy combined with a two-dimensional COSY methodology, by using a Bruker Avance 500 spectrometer operating at room temperature. The structural and morphological properties of the conjugates studied were examined with a transmission electron microscope (Technai T12) operating at 120 kV with a magnification of 52 k. High-resolution TEM images and diffraction analysis data were recorded with a Jeol 4000EX instrument operating at 400 kV with magnification of 200 KX. EELS spectra were recorded on a Hitachi HF-2000 field-emission-gun TEM instrument operating at 200 kV.

The room-temperature and low-temperature cw-PL spectra of the PbSe NQD–γ-Fe$_2$O$_3$ NP conjugate (suspended in either water or 2,2,4,4,6,8,8,-heptamethylnonane glassy solution) were obtained by exciting the samples with a Ti:sapphire laser, while the emission was recorded with an Acton monochromator equipped with a charge-coupled device (CCD). The PL spectra at low temperatures were recorded by introducing the sample into a magneto-optics Janis cryogenic Dewar, including a superconducting Halmontz coil that induced an external magnetic field up to 3 T. Lifetime measurements were performed by exciting the samples with a 4 ns Nd:YAG pulsed laser with a laser fluency of <2 mJ cm^{-2} and by detecting the delayed fluorescence with a Hammamatu photomultiplier tube, model H9170-75, operating in the near-infrared spectral regime with a time resolution of about 2 ns.

The magnetic properties of the PbSe NQD–γ-Fe$_2$O$_3$ NP conjugate structures were studied by using a field-shielded SQUID magnetometer MPMS$_2$ controlled by MultiVu software (Quantum Design Inc.). The samples were prepared by deposition of a colloidal solution of the individual NPs or of the NQD–NP conjugates in D$_2$O on a filter paper, and allowing evaporation of the solvent. The magnetization of the samples reported in the current study was always corrected for background response, and was associated with the contribution of the empty filter paper to the overall magnetization under the same experimental conditions. This correction was carried out by using the automatic background subtraction (ABS) method. The magnetization measurements used 6.3 mg of PbSe NQD–γ-Fe$_2$O$_3$ NP conjugate structures and 11.2 mg of γ-Fe$_2$O$_3$ NPs. The direct current (dc) mass magnetic susceptibility was measured versus the change in temperature from 2 K to room temperature, with an increment of $\Delta T = 2$ K. The initial cooling was done either in the presence of an external magnetic field with strength $H =$ 500 Oe (field cooled, FC) or in the absence of a magnetic field (zero field cooled, ZFC). The magnetic susceptibility dependence versus the strength of the external magnetic field was measured at a constant temperature, with a stability of $\Delta T < 0.005$ T, by varying the field strength in the range $-10\,000$ Oe $\leq H \leq 10\,000$ Oe.

Acknowledgements

The authors are indebted to the Russell Berrie Foundation for the contribution of the excellent infrastructure and to the donation of Matilda and Gabriel Barnett for the establishment of the Nanocrystalline Laboratory at the Technion, to Yehudit Schmidt from the Department of Chemical Engineering and the Center of Complex Fluids at the Technion in Haifa, Israel, for her assistance with the transmission electron microscopy, to Dr. Yong Ding from the School of Materials Science and Engineering at the Georgia Institute of Technology in Atlanta, Georgia, USA, for his assistance with the EELS measurements, and to Dr. Yael Balazs for assistance with the NMR measurements. L.F. acknowledges a Marie Curie Outgoing International Fellowship. This project was partially supported by the Israel Science Foundation, project Nos. 1009/07 and 650/06, and by a European Union Marie Curie International Reintegration Grant (IRG) No. 036577.

Keywords: conjugation · hydrogen bonds · magnetic properties · nanoparticles · quantum dots

[1] W. Shi, H. Zeng, Y. Sahoo, T. Y. Ohulchanskyy, Y. Ding, Z. L. Wang, M. Swihart, P. N. Prasad, *Nano Lett.* **2006**, *6*, 875.
[2] E. V. Shevchenko, D. V. Talapin, N. A. Kotov, O. Stephan, C. B. Murray, *Nature* **2006**, *439*, 55.
[3] H. Kim, M. Achermann, L. P. Balet, J. A. Hollingsworth, V. I. Klimov, *J. Am. Chem. Soc.* **2005**, *127*, 544.
[4] D. Wang, J. He, N. Rozenzweig, Z. Rozenzweig, *Nano Lett.* **2004**, *4*, 409.
[5] T. J. Yoon, J. S. Kim, B. G. Kim, K. N. Yu, M. H. Cho, J. K. Lee, *Angew. Chem.* **2005**, *117*, 1092; *Angew. Chem. Int. Ed.* **2005**, *44*, 1068..
[6] A. Santoni, G. Paolucci, G. Santoro, K. C. Prince, N. E. Christensen, *J. Phys. Condens. Matter* **1992**, *4*, 6759.
[7] A. P. Alivisatos, *J. Phys. Chem.* **1996**, *100*, 13226.
[8] C. R. Kagan, C. B. Murray, M. G. Bawendi, *Phys. Rev. B* **1996**, *54*, 8633.
[9] a) E. H. Sargent, *Adv. Mater.* **2005**, *17*, 515; b) S. Kim, Y. T. Lim, E. G. Soltesz, A. M. De Grand, J. Lee, A. Nakayama, J. A. Parker, T. Mihaljevic, R. G.

Laurence, D. M. Dor, L. H. Cohn, M. G. Bawendi, J. V. Frangioni, *Nat. Biotechnol.* **2004**, *22*, 93.
[10] E. Lifshitz, M. Brumer, A. Kigel, A. Sashchiuk, M. Bashouti, M. Sirota, E. Galun, Z. Burshtein, A. Q. Le Quang, I. Ledoux-Rak, J. Zyss, *J. Phys. Chem. B* **2006**, *110*, 25356.
[11] H. Du, C. Chen, R. Krishnan, T. D. Krauss, J. M. Harbold, F. W. Wise, M. G. Thomas, J. Silcox, *Nano Lett.* **2002**, *2*, 1321.
[12] B. L. Wehrenberg, C. Wang, P. Guyot-Sionnest, *J. Phys. Chem. B* **2002**, *106*, 10634.
[13] J. S. Steckel, S. Coe-Sullivan, V. Bulovic, M. G. Bawendi, *Adv. Mater.* **2003**, *15*, 1862.
[14] N. Gaponik, I. L. Radtchenko, M. R. Gerstenberger, Y. A. Fedutik, G. B. Sukhorukov, A. L. Rogach, *Nano Lett.* **2003**, *3*, 369.
[15] V. I. Klimov, J. A. McGuire, R. D. Schaller, V. I. Rupasov, *Phys. Rev. B* **2008**, *77*, 195324.
[16] B. H. Sohn, R. E. Cohen, *Chem. Mater.* **1997**, *9*, 264.
[17] S. Sun, C. B. Murray, *J. Magn. Magn. Mater.* **1999**, *85*, 4325.
[18] J. Popplewell, L. Sakhnini, *J. Magn. Magn. Mater.* **1995**, *149*, 72.
[19] K. Raj, B. Moskowitz, R. Casciari, *J. Magn. Magn. Mater.* **1995**, *149*, 174.
[20] R. S. Molday, D. Mackenzie, *J. Immunol. Methods* **1982**, *52*, 353.
[21] C. W. Jung, P. Jacobs, *Magn. Reson. Imaging* **1995**, *13*, 661.
[22] L. Etgar, E. Lifshitz, R. Tannenbaum, *J. Phys. Chem. C* **2007**, *111*, 6238.
[23] A. Olkhovets, R. C. Hsu, A. Lipovskii, F. W. Wise, *Phys. Rev. Lett.* **1998**, *81*, 3539.
[24] A. Kigel, M. Brumer, G. I. Maikov, A. Sashchiuk, E. Lifshitz, *Small* **2009**, DOI: 10.1002/smll.200801378.
[25] J. M. An, A. Franceschetti, A. Zunger, *Phys. Rev. B* **2007**, *76*, 045401.
[26] Y. M. Niquet, C. Delerue, G. Allen, M. Lannoo, *Phys. Rev. B* **2002**, *65*, 165334.
[27] R. C. O'Handley, *Modern Magnetic Materials*, Wiley-Interscience, New York, **2000**.
[28] D. Cui, J. Xu, T. Zhu, G. Paradee, S. Ashok, M. Gerhold, *Appl. Phys. Lett.* **2006**, *88*, 183111.
[29] E. Dubois, J. Chevalet, *Langmuir* **2003**, *19*, 10892.
[30] W. Zhang, A. O. Govorov, G. W. Brayent, *Phys. Rev. Lett.* **2006**, *97*, 146804.
[31] J. L. Dormann, D. Fiorani, E. Tronc, *Adv. Chem. Phys.* **1997**, *98*, 283.
[32] J. L. Dormann, L. Spinu, E. Tronc, J. P. Jolivet, F. Lucari, F. D'Orazio, D. Fiorani, *J. Magn. Magn. Mater.* **1998**, *183*, L255.
[33] J. L. Dormann, D. Fiorani, M. El Yamani, *Phys. Lett. A* **1987**, *120*, 95.
[34] W. F. Brown, *Phys. Rev.* **1963**, *130*, 1677.
[35] N. Ashcroft, N. Mermin, *Solid State Physics*, Holt, Rinehart, and Winston, New York, **1976**, p. 673.
[36] L. M. Malkinski, J. Q. Wang, J. B. Dai, J. Tang, *Appl. Phys. Lett.* **1999**, *75*, 844.
[37] M. Brumer, A. Kigel, L. Amirav, A. Sashchiuk, O. Solomesch, N. Tessler, E. Lifshitz, *Adv. Funct. Mater.* **2005**, *15*, 1111.
[38] W. W. Yu, J. C. Falkner, B. S. Shin, V. L. Colvin, *Chem. Mater.* **2004**, *16*, 3318.
[39] E. E. Larken, S. G. Grancharov, S. O'Brien, T. J. Deming, G. D. Stucky, C. B. Murray, G. A. Held, *Nano Lett.* **2003**, *3*, 1489.
[40] B. L. Frankamp, N. O. Fischer, R. Hong, S. Srivastava, V. M. Rotello, *Chem. Mater.* **2006**, *18*, 956.

Received: May 5, 2009
Published online on July 23, 2009

© 2009 Wiley-VCH Verlag GmbH & Co. KGaA, Weinheim